Proceedings of the International Association for Shell and Spatial Structures (IASS) Symposium 2009, Valencia
Evolution and Trends in Design, Analysis and Construction of Shell and Spatial Structures
28 September – 2 October 2009, Universidad Politecnica de Valencia, Spain
Alberto DOMINGO and Carlos LAZARO (eds.)

Seismic Risk Evaluation of Spatial Structures by using Grid Computing System

Shoji NAKAZAWA*, Shiro KATO[a], Ryoichi SHIBATA[b]

* Assoc. Prof. Department of Architecture and Civil Engineering,
Toyohashi University of Technology, Tempaku, Toyohashi 441-8580. Japan
E-mail : nakazawa@tutrp.tut.ac.jp

[a] Toyohashi University of Technology
[b] Gifu Natural College of Technology

Abstract

The present study propose a simple procedure to evaluate the seismic risk of the spatial structures by using grid computing system. As an example for calculating the seismic risk by using the system, numerical studies for single layer lattice domes supported by substructure implemented with buckling restricted braces are presented considering a simple rule for judging the damages of the structural and non-structural elements. The effectiveness of the system is discussed through the numerical example for dome structures.

Keywords: seismic risk, seismic fragility curve, grid computing system, dynamic response analysis, dome structure, buckling restricted brace

1. Introduction

In the areas of high seismic hazard, the necessity for anti-seismic reinforcement and seismic risk evaluation of spatial structures has been increasing [1]. Seismic risk analysis (SRA) [2,3] is a tool to quantify the seismic damage of an individual facility, aiming at providing information for decision making on risk mitigations of facilities.

In the present procedures, a seismic loss function (SLF) of a facility, which represents the relationship between the seismic expected loss and the ground motion level, is evaluated based on dynamic response analysis. A probabilistic seismic hazard curve (PSHC), which is an annual excess probability of maximum ground motion at a site, is also determined based on seismic environments. An annual expected loss and a seismic risk curve, which are important indices in seismic risk analysis, are obtained from SLF and PSHC. And a life cycle cost (LCC) of the facility is discussed from the annual expected loss. In order to evaluate the seismic risk, seismic fragility curves (SFCs) of structural components, which are main frames, braces and finishing materials, are determined based on the results of

damage investigations [4] or numerical studies. In the previous studies [3,5-7] on seismic risk evaluation of a residence, a gymnasium and a dome, SFCs of spatial structures have been calculated based on numerical results by elasto-plastic dynamic response analysis, since there is little damage investigation about gymnasia and domes.

A high performance computing is required in the study of risk analysis with many factors. A Grid Computing System [8] is a new and powerful method for realizing high performance computing. The system consists of an administrative host and many execution hosts. The system can provide a virtual massive parallel computer system by integrating many micro computers. The computing system can perform a vast set of structural analysis with in a moderate computing time and it can be effectively and parametrically applied to investigate seismic response characteristics. Accordingly, the system has an ability to be also applied to determine SFCs of structural components in seismic risk analysis. In our study, the seismic risk evaluation system by using Grid Computing is proposed, and the effectiveness of the system is discussed through a numerical example for dome structures.

2. Seismic risk analysis by using grid computing system

The calculation in present study is based on Grid Computing System [8] composed of micro computing units. The system can execute distributed parallel processing for vast jobs based on efficient schedule management. It can perform a many set of structural analysis within a moderate computing time and it can be effectively and parametrically applied to investigate structural characteristics. In our Grid System, the micro computers for daily jobs at laboratories are directed to the numerical analysis purpose. Therefore, the system is of much cost effective if introduced to many engineering offices.

A general system is shown in Fig.1, where a host computer is connected for control with following many execution-hosts through hubs. Each execution-host is composed of many micro computers which can perform real jobs. In the present situation at our laboratory, NSX- GRID System, which is called Numerical simulation for Structural engineering with eXtensity Grid Computing System, is already built. 75 computing units, which have 150 computer cores, are connected with the controlling hosts, and this system can perform 150 jobs simultaneously. About 500 times repetition of elasto-plastic response analysis is performed for seismic risk analysis of one structure, as described in section 3.2. The effectiveness of this system is examined by actually carrying out seismic risk analysis of a single layer lattice dome.

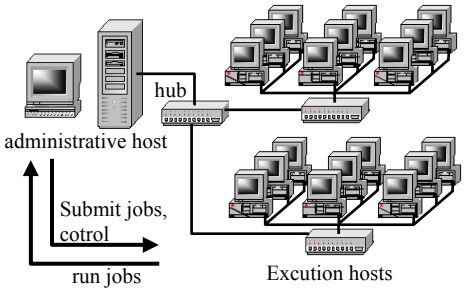

Fig.1 Grid computing system

3. Seismic response characteristics of Single layer latticed dome

3.1. Numerical models

A dome with a diameter of 100 meters is assumed for analysis as one of the typical examples for sport halls of medium size. The structure is shown in Fig.2, where the total building is divided here into two parts: the dome and the substructure supporting the dome. The substructure is composed of diagonal braces and vertical columns with wall finishing as non-structural covering material. The dome may be of double layer or single layer, and in this study it is assumed as a single layer steel lattice roof, where a ceiling of large area is finished inside the roof.

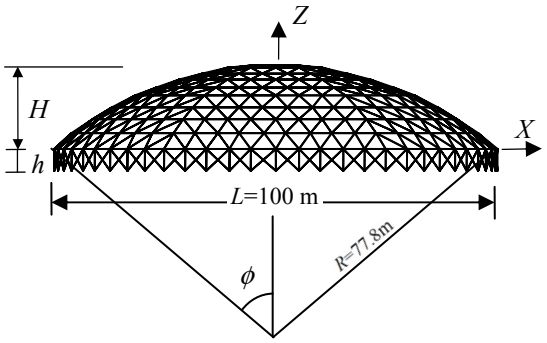

Fig.2 A steel single layer lattice dome supported by the substructure

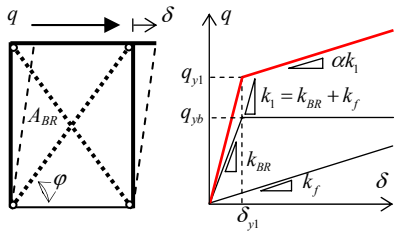

Fig.3 Replacement of brace hysteresis into equivalent bi-linear rule

3.1.1. Dome structure

The single layer lattice dome is composed of tubular steel members, and the cross sections of the members are assumed to be the same value as Dome D model in the reference [9]. A limitation is added that the members within the dome roof have a same diameter of 512mm and the diameter of tension ring is twice the diameter of the roof members. The members are proportioned for the thickness of tubular members in a way that the dome has a bearing capability to resist the two times dead load, P_{d0}=1470N/m^2 per unit area and also that it resists the additional static earthquake load ,P_{E0} , with 0.6 as the base shear coefficient defined at the dome base. The earthquake load P_{E0} is prepared using a linear earthquake response of dome under El Centro NS with a peak acceleration of $A_{\max}$=320cm/s^2. The total weight of the dome is assumed as W_t=17400kN including tension ring, and the weight of the wall is included as the mass of substructure. The elastic modulus E and yield strength σ_y are assumed as 2.05x10^{5}N/mm^2 and 235N/mm^2, respectively. The detail of members and other structural characteristics are abbreviated for brevity.

The bearing capacity is illustrated in Fig.4, where the load-displacement relationship is given at Node a. The result is based on an elasto-plastic buckling analysis of the Dome (α_{y0}=0.3, bi-linear) using a geometrically and materially nonlinear analysis [9]. From Fig.4,

it is verified that the dome satisfies the design requirement for dead load that the dome should endure the load twice the dead load. Other cases with a different value of α_{y0} are almost same and abbreviated in this paper.

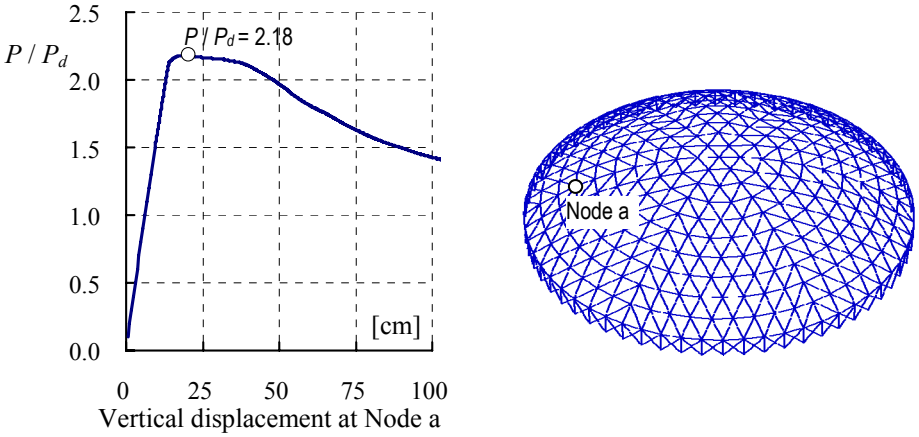

Fig.4 Bearing capacity of dome under dead load

3.1.2. Substructure and numerical parameters

The numerical parameters of the brace which constitutes the substructure are shown in Table 1. α_{y0} is the design base shear coefficient for braces. A_{BR} is the area of each brace element, K_{BR} is the shear rigidity of one set of braces as given in the right part of Fig.3, and κ represents the elastic shear rigidity of other structural element except for the brace element, being assumed 0.2 as the ratio to the brace rigidity. Δ_{y1} is the story drift for initial yield. The hysteresis of the brace are assumed a bi-linear type supposing a buckling restricted brace. The axial rigidity of columns is assumed very large, and the vertical displacements at column tops are fixed zero in the analysis.

Table 1 Bracing elements

	α_{y0}	σ_y (N/mm^2)	A_{BR} (cm^2)	K_{BR} (N/cm)	κ = K_f / K_{BR}	Δ_{y1} (cm)
C02B	0.2	235	2.811	11.78	0.2	0.834
C03B	0.3		4.216	17.67		
C04B	0.4		5.622	23.56		
C05B	0.5		7.802	29.45		

α_{y0} : design base shear coefficient for braces, σ_y : yield stress, A_{BR} : sectional area of the brace,
Δ_{y1} : story drift for initial yield

3.2. Input Ground motions

To investigate the fragility of a real dome requires a set of earthquake motions that are selected by reflecting the site seismic activity. However, the dome studied in this paper is only conceptual. Accordingly, artificial earthquake motions are prepared based on the design spectrum of Japan Building Code [10] corresponding to a soil surface for the ordinary soil condition of the kind II. The spectrum for the serviceability limit level is specified as λ_E =1.0. For investigation of the fragility of dome, fifty artificial ground earthquake motions are simulated using phases drown from fifty recorded earthquake accelerations. They are El-Centro NS, Taft EW and other recorded accelerations that are often applied in aseismatic design. Roughly the average peak acceleration for λ_E=1 corresponds to 115 cm/s^2. The simulated acceleration spectrum is shown in Fig.5.

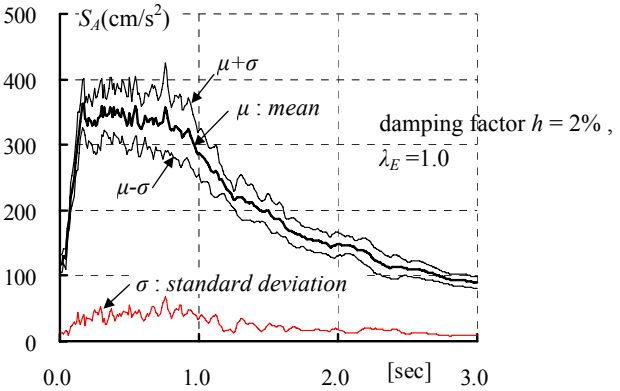

Fig.5 Mean and standard deviation of acceleration response spectra of seismic motions

3.3. Seismic response characteristics

Average acceleration method of Newmark-β scheme with β=1/4 is used for numerical integration, and the time interval for response calculation Δt is 0.002sec. The Rayleigh damping matrix is used and damping factors of 2% for the two dominant vibration modes which have a significant participation factor is assumed.

Fig.6 illustrates the relations between maximum responses and seismic intensity λ_E in case of C30B. The maximum value of vertical displacement, horizontal acceleration and vertical acceleration of dome, d_{DV}, A_{DH}, A_{DV} are shown. The maximum values of horizontal displacement and horizontal acceleration at column top, d_{SH} and A_{SH} , are also shown. Fig6 (f) illustrates the maximum cumulative plastic deformation ratio η of braces in substructure. As shown in Figs.6, maximum responses increase with an increase in λ_E. Due to the difference of input earthquake motions, the maximum responses for λ_E vary over a wide range.

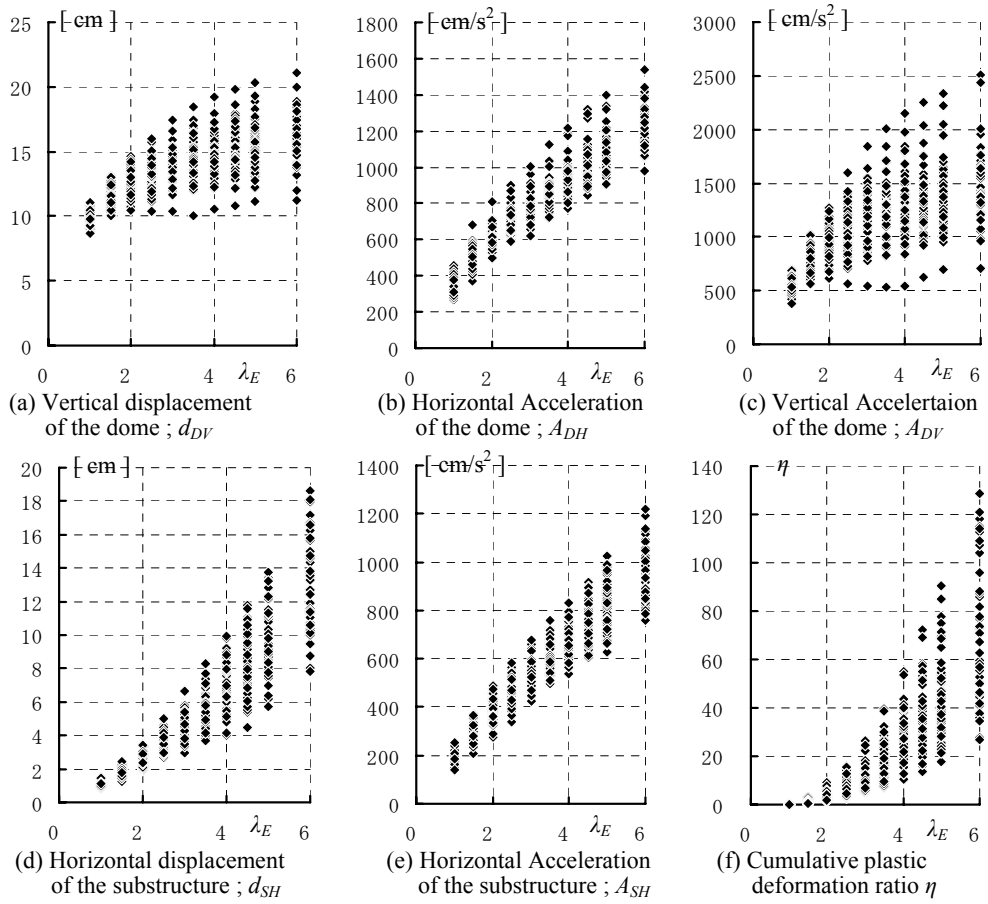

(a) Vertical displacement of the dome ; d_{DV}
(b) Horizontal Acceleration of the dome ; A_{DH}
(c) Vertical Accelertaion of the dome ; A_{DV}
(d) Horizontal displacement of the substructure ; d_{SH}
(e) Horizontal Acceleration of the substructure ; A_{SH}
(f) Cumulative plastic deformation ratio η

Fig.6 Relationship between maximum responses and seismic intensity λ_E (C03B, α_{y0}=0.3)

4. Example of seismic risk analysis of dome structures

4.1. The damage evaluation index and its criteria of a structural element

As a composition of the dome, we roughly divide domes into the following four compositions ; 1) structural elements for a dome roof, 2) non-structural elements on a dome roof, 3) structural elements of a substructure and 4) non-structural elements on a substructure. The damage of the equipments is not taken into consideration in this research.

The damage on the structural elements of the dome is assumed to be evaluated by the maximum vertical displacement of the dome, d_{DV}. Several damage states (DS) for defining the degree of damage are set up as shown in Table 2. The criteria of the damage states and damage ratio R_{DS0} (DS) of structural element of the dome are also listed.

The non-structural elements of the dome represents a finishing material on the roof. The damage is assumed to be estimated by the maximum horizontal and vertical accelerations of dome, A_{DV} and A_{DV}. The criteria of the damage states and damage ratio of non-structural elements of dome R_{DN0} are assumed with reference to the reference [10] as shown in Table 3.

The structural elements of the substructre represent a set of buckling restrained brace, and the damage is assumed to be estimated by the cumulative plastic deformation ratio η of braces. The non-structural elements of the substructure represent a finishing material, and the damage is estimated by maximum story drift angle of the substructure Δ. The damage ratios of structural and non-structural elements, which are expressed as R_{SS0} and R_{SN0}, are also listed in Table 4 and Table 5, respectively.

At present, the proposed rules are assumed presumably in this study, accordingly it is surely necessary to say that more realistic data is required for more realistic and precise evaluation of the fragility.

Table 2 Damage state and damage ratio of the structural elements of the dome

Criteria	$d_{DV} < d_{DV1}$	$d_{DV1} < d_{DV} < d_{DV2}$	$d_{DV2} < d_{DV} < d_{DV3}$	$d_{DV} > d_{DV3}$
Damage State ; *DS*	A	B	C	D
$R_{DS0}(DS)$	0.0	0.25	0.50	1.0

d_{DV} : maximum vertical displacement of the dome, d_{DV1} = 12 cm, δ_{DV2} = 24 cm, δ_{DV3} = 36 cm

Table 3(a) Damage state and damage ratio of the non-structural elements of the dome

	$A_{DV} \leqq A_{DV1}$	$A_{DV1} < A_{DV} \leqq A_{DV2}$	$A_{DV2} < A_{DV} \leqq A_{DV3}$	$A_{DV} > A_{DV3}$
$A_{DH} \leqq A_{DH1}$	A	B	C	D
$A_{DH1} < A_{DH} \leqq A_{DH2}$	B	B	C	D
$A_{DH2} < A_{DH} \leqq A_{DH3}$	C	C	C	D
$A_{DH} > A_{DH3}$	D	D	D	D

A_{DV}, A_{DH} : maximum vertical and horizontal acceleration of the dome
$A_{DV1} = A_{DH1}$ = 800cm/s^2, $A_{DV2} = A_{DH2}$ = 1200cm/s^2, $A_{DV3} = A_{DH3}$ = 1600 cm/s^2

Table 3(b) Damage state and damage ratio of non-structural members of dome

Damage State ; *DS*	A	B	C	D
$R_{DN0}(DS)$	0.0	0.25	0.50	1.0

Table 4 Damage state and damage ratio of the structural elements of the substructure

Criteria	$\eta \leqq 100$	$\eta_1 < \eta \leqq \eta_2$	$\eta_2 < \eta \leqq \eta_3$	$\eta > \eta_3$
Damage State ; *DS*	A	B	C	D
$R_{SS0}(DS)$	0.0	0.25	0.50	1.0

η: Cumulative plastic deformation ratio, η_1 = 100, η_2 = 200, η_3 = 300

Table 5 Damage state and damage ratio of the non-structural elements of the substructure

Criteria	$\Delta \leqq \Delta_1$	$\Delta_1 < \Delta \leqq \Delta_2$	$\Delta_2 < \Delta \leqq \Delta_3$	$\Delta > \Delta_3$
Damage State ; *DS*	A	B	C	D
$R_{SN0}(DS)$	0.0	0.25	0.50	1.0

Δ : maximum story drift angle of the substructure, Δ_1 = 1/100, Δ_2 = 1/50, Δ_3 = 1/30

4.2. Seismic fragility curve (SFC)

SFC is the probability of failure at a certain seismic intensity, λ_E. Generally, when the probability distributions of load and resistance are known, probability of failure p_f can be calculated based on a theory of structural reliability [2,3]. The SFC of spatial structures based on the theory are illustrated in the previous studies [5,6].

On the other hand, SFC is calculated more simply and directly in this study. Seismic response analyses subjected to 50 earthquake motions are carried out, and maximum responses are analyzed on each seismic intensity, λ_E. For example, when asking for the SFC of the structural elements of the dome, based on the damage criteria of Table 2, the occurrence probability of each damage state is directly calculated from the result of maximum vertical displacement of the dome, d_{DV}, obtained from the numerical analysis. Fig.7(a) illustrates the example of occurrence probability of each damage state of non-structural element of the dome in the case of C30B model. SFC obtained from probability of occurrence is also shown in Fig.7(b).

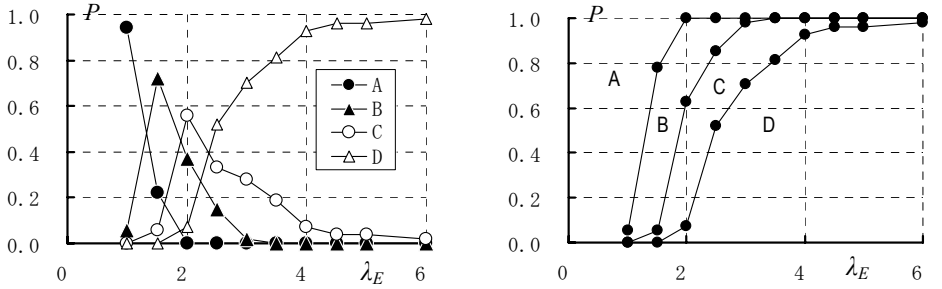

(a) Occurrence probability (b) Seismic fragility curve (SFC)

Fig.7 Occurrence probability of each damage state (A, B, C, D) and SFC of non-structural element of the dome in the case of C30B model

4.3. Expected Damage Ratio

$R_{DS}(\lambda_E)$ denotes a expected damage ratio of the structural element of the dome corresponding to seismic intensity λ_E, and it is calculated as follows,

$$R_{DS}(\lambda_E) = \sum\left[R_{DS0}(DS)\times p_{DSi}(\lambda_E)\right] \quad ; \quad DS = A,B,C,D \tag{1}$$

Here, $R_{DS0}(DS)$ and $p_{DSi}(\lambda_E)$ are the damage ratio and the occurrence probability of damage state DS. The expected damage ratios of other components are similarly calculated, and the expected damage ratios are illustrated in Fig.8. The expected damage ratio increases with the increase in seismic intensity, λ_E. R_{DS} and R_{DN}, which are the expected damage ratio of the structural and non-structural elements of the dome, tend to increase with an increase in the yield shear coefficient of substructure, α_{y0}. On the other hand, the expected damage ratio of the structural and non-structural elements of the substructure tends to decrease with an increase in α_{y0}. It is confirmed that the damage ratio of the dome has a relation of a trade-off to the damage ratio of the substructure.

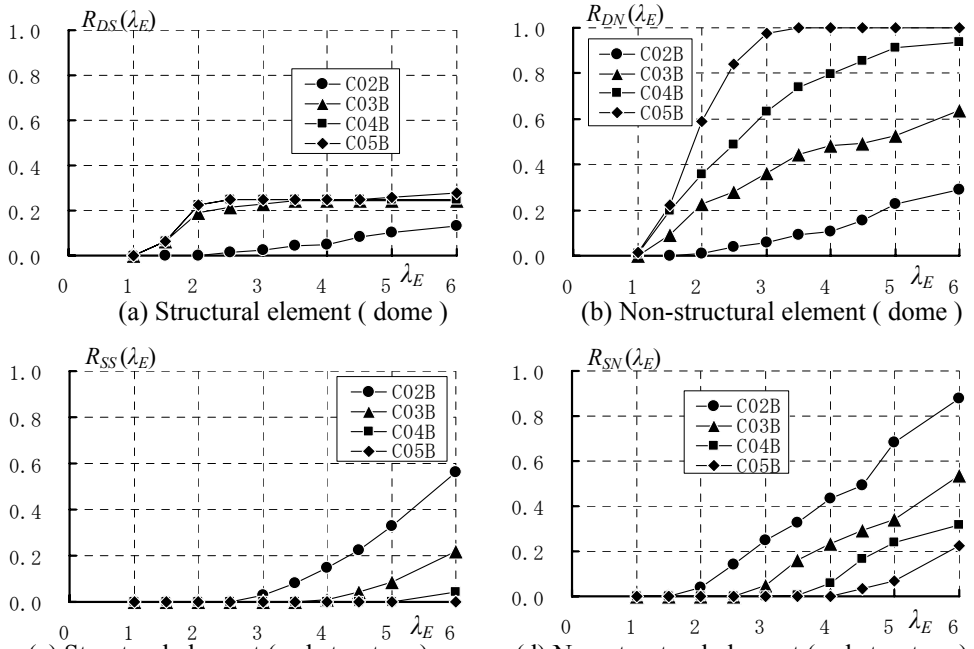

(a) Structural element (dome) (b) Non-structural element (dome)

(c) Structural element (substructure) (d) Non-structural element (substructure)

Fig.8 Expected damage ratio

4.4. Seismic Loss Function

A seismic loss function (SLF) represents the relation between the seismic expected loss and the ground motion level. The seismic expected loss is the product of the probability of damage state and its corresponding loss amount associated with the state. Although the seismic loss function is calculated using an event tree modeling, SLF is simply calculated in the following procedures. The seismic loss of the whole structure, $C_{SL}(\lambda_E,k)$, corresponding to input earthquake motion k of seismic intensity λ_E is calculated for simplification.

$$C_{SL}(\lambda_E,k) = \begin{cases} \sum_J \left[C_{J0} \times R_J(\lambda_E,k) \right] \; ; \; J = DS, DN, SS, SN \\ 1.0 \end{cases} \tag{1}$$

Here, the damage of each composition is assumed to be mutually independent, and $C_{SL}(\lambda_E,k)$ is calculated from the alignment sum of the seismic loss of each component. However, when the damage state of the structural element is "D", it conludes that the whole structure is collapsed and $C_{SL}(\lambda_E,k)$ is assumed 1.0 unconditionally. C_{DS0}, C_{DN0} , C_{SS0} and C_{SN0} are assumed to be here 0.4, 0.2, 0.3 and 0.1 in this study. Since SLF is given as an expected value of $C_{SL}(\lambda_E,k)$, the seismic loss function, $C_{ESL}(\lambda_E)$, is calculated as

$$C_{ESL}(\lambda_E) \;=\; E\left[\, C_{SL}(\lambda_E,k) \,\right] \;=\; \frac{1}{N}\sum_{k=1}^{N}\left[\, C_{SL}(\lambda_E,k) \,\right] \tag{2}$$

in which N expresses the number of input earthquake motions. Moreover, the standard deviation $\sigma_{SL}(\lambda_E)$ of $C_{SL}(\lambda_E,k)$ can be calculated as follows.

$$\left(\sigma_{SL}(\lambda_E)\right)^2 \;=\; Var\left[\, C_{SL}(\lambda_E,k) \,\right] \;=\; \frac{1}{N}\sum_{k=1}^{N}\left\langle C_{SL}(\lambda_E,k) \;-\; C_{ESL}(\lambda_E)\right\rangle^2 \tag{3}$$

Fig.9 shows the examples of the seismic loss function, $C_{ESL}(\lambda_E)$. $C_{SL}(\lambda_E,k)$ and standard deviation $\sigma_{SL}(\lambda_E)$ are also illustrated in Fig.9. $C_{SL}(\lambda_E,k)$ varies due to the difference of earthquake motions. $C_{ESL}(\lambda_E)$ increases with an increase in λ_E. $C_{SL}(\lambda_E,k)$ becomes 1.0 in the several cases of C02B model subjected to severe earthquake motions (λ_E =5 and 6), since the damage state of the structural elements of the substructure becomes “collapse”.

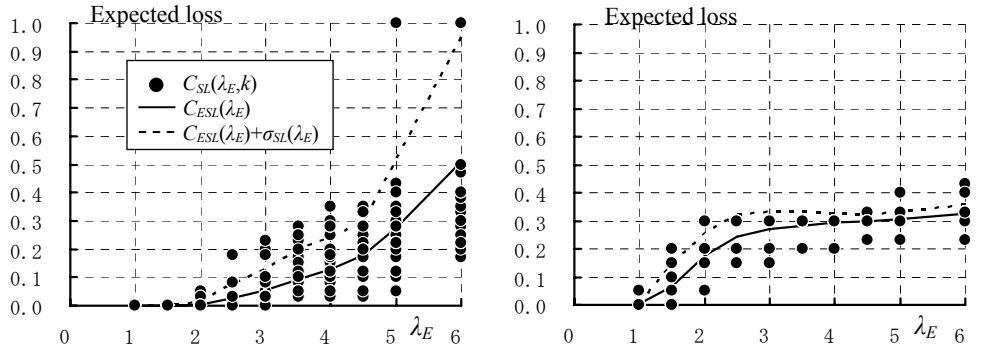

(a) C02B (C_y=0.2) (b) C05B (C_y=0.5)

Fig.9 Seisimic loss function ; $C_{ESL}(\lambda_E)$

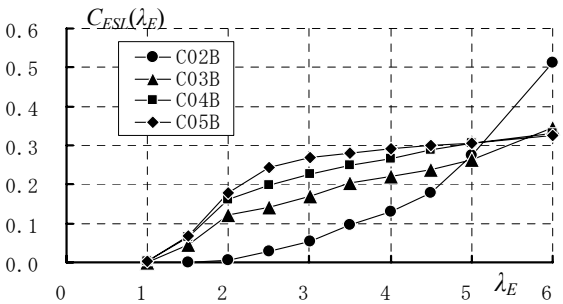

Fig.10 Comparison of the expected seismic loss $C_{ESL}(\lambda_E)$ on yield shear coefficient α_{y0}

Fig.10 shows the relation between the normal expected seismic loss $C_{ESL}(\lambda_E)$ and λ_E. When λ_E is smaller than 5.0, $C_{ESL}(\lambda_E)$ tends to become decrease with an increase in α_{y0}. The damage of the non-structural elements of the dome contributes to the expected loss greatly

as shown in Fig.8. Since the input energy to the dome increases with an increase in α_{y0}, it is considered that the damage of the non-structural elements of the dome increases with an increase in α_{y0}. On the other hand, when λ_E is greater than 5.0, $C_{ESL}(\lambda_E)$ in the case of α_{y0}=0.2 becomes the largest. In this case, the damages to the structural and non-structural elements of the substructure has large influence on $C_{ESL}(\lambda_E)$.

4.5. Seismic Hazard Curve and Life Cycle Cost

A probabilistic seismic hazard curve (PSHC) is an annual excess probability of maximum ground motion at a site. In a seismic risk analysis, given the probabilistic seismic hazard curve at the facility site, the annual expected seismic loss, S_{ASL}, is obtained by convoluting the seismic loss function with the probabilistic seismic hazard curve [2].

$$S_{ASL} = \int_0^\infty \left\langle F_{SL}(a) \frac{d\,H(a)}{da} \right\rangle da \tag{4}$$

Here, $F_{LS}(a)$ and $H(a)$ represent the seismic loss function and the seismic hazard curve at ground motions level a, respectively. Since the seismic risk function is given with a discrete function in this study, S_{ASL} is calculated from the following approximations.

$$S_{ASL} \approx \sum_i \left\langle C_{ESL}(\lambda_{Ei}) \times p(\lambda_{Ei}) \right\rangle \tag{5}$$

Here, $C_{ESL}(\lambda_{Ei})$ is the seismic loss function calculated from Eq.(2), and $p(\lambda_{Ei})$ is an annual occurrence probability of the earthquake motion at seismic intensity λ_{Ei}. Using of the annual expected seismic loss, S_{ASL}, it is possible to calculate the Life Cycle Cost of the object structure and to evaluate the effectiveness of retrofit proposal based on the discounted cash flow method [6].

5. Conclusion

The present study has proposed a simple procedure to evaluate the seismic risk of the spatial structures by using a grid computing system. As an example for calculating the seismic risk by using the system, numerical studies for single layer lattice domes supported by substructure with buckling restricted braces were presented considering a simple rule for judging the damages of the structural and non-structural elements.

First, the damage states and its criteria of the structural and non-structural elements were assumed. At present, the proposed rules were assumed presumably in this study, accordingly it is surely necessary to say that more realistic data is required for more realistic and precise evaluation of the fragility. Second, the calculation method of the seismic fragility curves and the seismic loss function based on the results of elasto-plastic seismic response analysis is explained. In order to carry out many response analyses quickly, the grid computer system was sysyematized, and the effectiveness of grit computer systems was verified. Finally, the relation between the normal expected seismic loss and yield shear coefficient α_{y0} of the substructure was illustrated. It was clearly revealed that the damage of the dome had a relation of a trade-off to the damage of the substructure and the

yield shear coefficient of the substructure which makes an expected loss small was also discussed.

Acknowledgement

The first author is grateful for the partial supports as a Grand-in-Aid for Young Scientists (B) No.20760371 given by the Ministry of Education, Science, Sports and Culture of Japanese Government.

References

[1] T.Takeuchi, S.D.Xue, S.Kato, T.Ogawa, M.Fujimoto and S.Nakazawa, *Recent Developments in Passive Control Technologies for Spatial Metal Structures*, Proc. of IASS-APCS 2006 Symposium, 2006, DR18.

[2] M.Mizutani, *Basic methodology of a seismic risk management procedure*, ICOSSAR '97, Vol.3, 1997, 1581-1588.

[3] M.Ooi, M.Mizutani, S.Yoshida, A.Nobata, K.Tanouchi and H.Fujiwara, *Study on Seismic Fragilities of Categorized Wooden Houses*, Technical Note of the National Research Institute for Earth Science and Disaster Prevention, No.250, 2004.

[4] K.Kawaguchi and Y.Suzuki, *Damage Investigations of Public Halls in Nagaoka City After Nigata-Chuetsu Earthquake 2004 in Japan*, Proc. of IASS2005, 2005, 421-428.

[5] S.Nakazawa, T.Shima, I.Tatemichi, S.Kato and K.Hirano, *Evaluation for Seismic Risk Based on Damage Ratio and Seismic Resistance of Spatial Structures*, IASS-APCS 2006 Symposium, 2006, AO16.

[6] S.Nakazawa, S.Kato, K.Hirano, *Methodology to Evaluate the Effectiveness of Retrofit Proposal Based on the Discounted Cash Flow Method*, IASS 2007 Symposium, PN368, Venice, Italy, 2007.

[7] S.Kato and S.Nakazawa, *Seismic risk Analysis of large lattice dome supported by buckling restrained braces*, IASS-IACM2008, Cornell University, Ithaca, USA, 2008.

[8] R.Shibata, S.Shimaoka, S.Kato, H.Murakami, S.Nakazawa, T.Sugiyama and H.Okubo, *Optimal Parameter Finding Based on Grid Computing System for Tuned Mass Dampers Applied to a Transmission Tower*, ISEC-03, 2005.

[9] S.Kato, S.Nakazawa and Y.Niho, *Seismic Design Method of Single Layer Reticular Domes with Braces Subjected to Severe Earthquake Motions*, APCS2000, 2000, Seoul, Korea, 131-140.

[10] M. Midorikawa, *Performance-Based Seismic Design Provisions for Buildings in Japan*, IASS 2005 Symposium, 2005, 307-316.

[11] Federal Emergency Management Agency, *HAZUS99 technical manual*, Washington, D.C., NY, 1999.